A Compact Size Capacitive Load Dual Band Planar Inverted-F Implant Antenna for Biomedical Services

Sanaa Salama (sanaa.salama@aaup.edu)
Arab American University https://orcid.org/0000-0001-9480-6985
Duaa Zyoud
Arab American University
Ashraf Abuelhaija
Applied Science Private University

Research Article

Keywords: implant antenna, capacitive load, compact size, SAR, and radiation patterns

Posted Date: June 13th, 2022

DOI: https://doi.org/10.21203/rs.3.rs-1631065/v1

Version of Record: A version of this preprint was published at Wireless Personal Communications on April 1st, 2023. See the published version at https://doi.org/10.1007/s11277-023-10396-2.

Abstract

In this work a compact size capacitive load dual band planar inverted-F implant antenna is presented. The suggested antenna is modeled on RO3010 substrate that has a thickness of 2 mm, dielectric constant of 10.2, and tangent loss of 0.0023 to operate at both the Medical Implant Communications Services (MICS) and Industrial, Scientific, and Medical (ISM) bands. A capacitive load is inserted between the patch and the ground plane to get a dual band and compact size implant antenna. The antenna size is 20× 12×2 mm^3. The antenna designed in this work operates at 402MHz with a return loss of -23.23dB over a frequency band [397.15-409.4MHz] for MICS band and operates at 2.42GHz with a return loss of -20dB over a frequency band [2.37-3GHz] for ISM band. The simulated gain is -27.52dBi at 402MHz for MICS band and − 1.85dBi at 2.42GHz for ISM band. The proposed antenna has a good performance inside three-layered tissue model. The Computer Simulation Technologies (CST) Microwave studio is used to model and simulate the proposed antenna.

1. Introduction

Recently, Implant Medical Devices (IMDs) are commonly used for biomedical purposes. The key component in IMDs is the implant antenna that used to transmit and receive electrical signal between the human body and external monitoring system. Because the implantable antennas are inserted inside the human body, many factors have to be considered such as compact size, patient safety, and radiation efficiency. Several techniques are used for antenna miniaturization purposes: in [1-3], substrate and superstrate with a high dielectric constant were used to minimize the antenna size. In [4-9], a short-circuited pin was inserted between the radiating conductor and the ground for antenna size miniaturization. Another technique is patch meandering used for antenna size reduction, [10-15]. The current path is increased by meandering the patch. In [16], a flexible dual band circular ring slot implant antenna with a compact size was proposed. An array of 2×2 metamaterial with Epsilon very large property was printed on the superstrate of the implant slot antenna. The idea behind metamaterial technique is to get gain enhancement (3dB gain enhancement was obtained at the operating frequency of 2.45GHz). A miniaturized implantable wideband antenna was developed in [17] to work at Human Body Communication (HBC) band. Helical copper foils are used to obtain a wideband antenna. The copper radiating element is forming on two layers of flexible magnet sheet to get a miniaturized antenna.

This work is an expansion to what we started in [6] and [7], where is [6] a single band planar inverted-F implant antenna was built and optimized to cover the MICS band with a size of (28×36×2 mm^3). While in [7], to obtain a dual band implant antenna, a planar inverted-L section is added. The L-section dimensions are optimized to cover the ISM band in addition to the MICS band that is covered by the planar inverted-F section. The proposed antenna in [7] is of a size (27× 19×2 mm^3). In this work, to obtain a dual band implant antenna operates at both MICS and ISM bands with further size reduction, the planar inverted-L section in [7] is replaced by a capacitive load inserted between the radiating conductor and the ground. The proposed implant antenna is designed and simulated in Computer Simulation Technologies (CST) Microwave studio. The paper is structured as follows; in section II, the antenna configuration is presented.

In section III and IV, simulation results and discussion are presented respectively. Simulated return loss at different antenna depths and for different biocompatible layer thickness is given in section V. Finally, conclusions are given in section VI.

2. Antenna Configuration

The implant antenna presented in this work is built to be a compact size dual band planar inverted-F implant antenna by inserting a capacitive load between the radiating conductor and the ground. The planar inverted L section in [7] is removed and the short-circuited pin in the planar inverted F section is replaced by a capacitive load. The antenna geometry is shown in Fig.1. The capacitive load value, the feed point position with respect to the capacitive load, and the planar inverted-F dimensions are all optimized such that both MICS and ISM bands are covered. The antenna dimensions are 20× 12× 2 mm^3. The capacitive value is 36pF, and a substrate with high dielectric constant; RO3010 with ε_r= 10.2, and thickness of 2mm; is used. A size reduction of 53.2% is obtained compared with the antenna size in [7], while a size reduction of 76.2% is obtained compared with the antenna size in [6]. In addition to the size reduction, the proposed antenna still supports both MICS and ISM bands. The implant antenna is fed by 50 Ohm source impedance. In this design, safety issues are considered to avoid any direct contact between the conducting material modeling by the radiating conductor and the human body.

To satisfy this purpose an Alumina superstrate with (ε_r = 9.4, tanδ = 0.006, and thickness 0.1mm) is used. The superstrate thickness is another parameter in our design that required to be optimized. In the optimization, the pre-defined goals are the dual bands (MICS and ISM) in addition to the further size reduction compared to that obtained in [6] and [7].

2.1 Three-Layer Tissue Model: CST Microwave studio is used to design and simulate the proposed antenna. For simulation, three-layer tissue model is designed consisting of skin of thickness 2 mm, fat of thickness 4 mm, and muscle of thickness 8 mm. The antenna is inserted in the muscle layer at a distance of 8 mm from the skin-air interface and a distance of 2 mm from the fat-muscle interface. Electrical properties of the skin, fat and muscle tissues in Table 1 are used in the design. A phantom of size 70×60×14 mm^3 is used to represent the model for the implant antenna under human chest. Figure 2 shows the average-thickness of three-layer tissue model. The skin, fat, and muscle are modeled in CST as a dielectric dispersion. The dielectric constant and conductivity values in Table 1 are inserted at both 402 MHz and 2.45 GHz to model the three-layer human tissue at both MICS and ISM bands. Where the dielectric constant value decreases by increasing the frequency, while the opposite is for the conductivity, [18] and [19].

Table 1. Electrical properties (permittivity, ε_r, conductivity, σ, loss tangent) of skin, muscle, and fat layer at MICS and ISM bands, [3].

Biological tissues	MICS band			ISM band		
	ε_r	σ(S/m)	tanδ	ε_r	σ(S/m)	tanδ
Skin	46.7	0.69	0.79	38.1	2.27	0.33
Muscle	57.1	0.79	0.62	52.7	1.73	0.24
Fat	5.58	0.04	0.32	5.28	0.10	0.14

3. Simulation Results

The return loss of the implant antenna for MICS band is shown in Fig.3a. while the return loss for ISM band is shown in Fig.3b. In addition, the simulated surface current density and electric field intensity at 402 MHz for the MICS band and at 2.42 GHz for the ISM band are shown respectively in Fig.4 and Fig.5. Simulated far-field patterns are shown in Fig.6 for the azimuth pattern (theta = 90^o) and the elevation pattern (phi = 0) at 402 MHz and 2.42 GHz respectively.

4. Discussion and Analysis of the Results

As could be noticed from Fig.3, the presented antenna is a dual band antenna. It covers a frequency band of 12.25 MHz [397.15-409.4 MHz] for MICS band with a return loss of -23.23 dB at 402 MHz. For the ISM band it covers a wide bandwidth of 630 MHz [2.37-3.00 GHz] with a return loss of -20dB at 2.42 GHz. A very good bandwidth enhancement is obtained, especially at the ISM band, due to the capacitive load effect in addition to 53.2% size reduction compared to the results in [7]. A size reduction of 76.2% is obtained compared to the results in [6]. The bandwidth enhancement at MICS and ISM band is calculated to be 23.3% and 87.3% respectively compared to the achieved bandwidth for the planar inverted F-L implant antenna in [7].

Human safety is an essential issue, so the average Specific Absorption Rate (SAR) value is very important in the design of biomedical antennas. The SAR value measures the absorbed power by a unit mass of biological tissue. The optimal SAR value is less than 1.6 W/Kg for C95.1-1999 system and less than 2 W/kg for C95.1-2005. For our design, the simulated SAR value based on 1 W input power at 402 MHz is 145.13 W/kg for 1g model and 42.56W/kg for 10g model. Similarly, the simulated SAR value at 2.42 GHz is 135.29 W/kg for 1g model and 41.87W/kg for 10g model. To be within the optimal values for the SAR, the maximum input power has to be reduced to 11mW (1 g) and 46.98 mW (10g) at 402 MHz for the MICS band. For the ISM band, the peak input power has to be reduced to 11.82mW (1 g) and 47.7 mW (10g) at 2.42 GHz.

At 402 MHz, the highest current density is mostly focused at the center, which means that the half-wavelength mode is excited. While at 2.42 GHz, the current peak values are mostly focused at the edges of the structure, which means that the full-wavelength mode is excited, Fig.4. For the electric-field intensity, it has its peak value on the center of the structure at 402 MHz. While the field peak values occur on the edges at 2.42 GHz as Fig.5 shows.

The antenna far-fields shown in Fig.6 are mostly directed away from the three-layer body model for both bands. The radiation pattern for the ISM band shows a null at $theta=\pm\pi/4$. The calculated gain for MICS band at 402 MHz is -27.52dBi and for the ISM band at 2.42 GHz is -1.85dBi. Low gain is a drawback in the design of the implantable antennas and a lot of researches focus on the gain enhancement techniques, [16], and [20-23]. A summary of the results obtained by this work in comparison to other works is given in Table 2.

5. Parametric Study

The simulated return loss for both MICS and ISM band at different implantable antenna depths is studied, Fig.7a, and Fig.7b respectively. The depth of the antenna for MICS band affects the matching at 402MHz, while for ISM band, the antenna depth affects both resonant frequency and the bandwidth. In addition, the simulated return loss for both MICS and ISM band at different biocompatible layer thickness is studied, Fig.8a, and Fig.8b respectively.

Table 2

A summary of the results obtained by this work in comparison to other works

Ref.	Antenna size	Frequency bands	Gain (dBi) MICS ISM	Substrate
[3]	14×17×0.25 mm^3	MICS, ISM	-33 -16	Roger-RT6010
[6]	24×32×2 mm^3	MICS	-18 –	Rogers-RO3010
[7]	27× 19×2 mm^3	MICS, ISM	-30.14 2.45	Rogers-RO3010
[8]	14×14×1.27 mm^3	MICS, ISM	-46 -19	Rogers-RO3010
[11]	Loop antenna of radius 5.5 mm and height 0.635 mm	MICS, ISM (902MHz)	-35.6 -26.3	Rogers-RO3010
[16]	10×10×0.4 mm^3	ISM	– -12	Kapton polyimide
This work	20× 12×2 mm^3	MICS, ISM	-27.52 -1.85	Rogers-RO3010

For MICS band, the resonant frequency increases by increasing the biocompatible layer thickness. For ISM band, the resonant frequency still the same for biocompatible layer thickness of 0.1mm and 0.15mm. At 0.2mm thickness, the resonant frequency is shifted to the right by 51MHz.

6. Conclusions

This paper represents a capacitive load dual band planar inverted-F antenna designed for biomedical purposes. The antenna with the three-layer human tissue model is designed and simulated using CST. The proposed antenna operates for both MICS band at 402MHz [397.15-409.4MHz] and ISM bands at 2.42GHz [2.37-3GHz] with a compact size of dimensions 20×12×2 mm^3. The antenna is modeled on RO3010 substrate and covered with an Alumina superstrate to guarantee safety issues for human body. In this paper by inserting a capacitive load, then a dual-band antenna is obtained with no need for a parasitic element. In addition, further size reduction is obtained. The presented antenna works for MICS band at 402MHz with a return loss of -23.23dB and for ISM band at 2.42GHz with a return loss of –20dB. The simulated gain is found as -27.52dBi at 402MHz and -1.85dBi at 2.42GHz. Low gain values can be considered as a challenge in the design of implantable antennas. To overcome this issue, several techniques could be used and this will be discussed as a future work.

For safety issue, the peak input power is required to be less than 11 mW (1 g) and 46.98mW (10g) at 402 MHz for the MICS band and 11.82mW (1 g) and 47.7mW (10g) at 2.42 GHz for the ISM band. The far-field patterns for both bands are mostly directed away from the body.

Declarations

Conflicts of Interest Statement: Authors certify that they have NO affiliations with or involvement in any organization or entity with any financial interest (such as employment, consultancies, stock ownership, honoraria, paid expert testimony, patent applications/registrations, and grants or other funding.

Availability of data and material: Data sharing not applicable to this article as no datasets were generated or analysed during the current study.

Funding: there is no funding for this research.

References

1. A. Kiourti and K. S. Nikita, “A Review of Implantable Patch Antennas for Biomedical Telemetry: Challenges and Solutions,” *IEEE Antennas Propagation Magazine*, Vol.54, No.3, pp-210-228, 2012.
2. A. Damaj, S. Abou Chahine and I. Damaj, "The Design and Implementation of Electrically Small Reconfigurable Patch Antennas," in *GCC Conference and Exhibition (GCC),* 2011.
3. A. Basir, A. Bouazizi, M. Zada, A. Iqbal, S. Ullah, U. Naeem, "A Dual-Band Implantable Antenna with Wide-Band Characteristics at MICS and ISM Bands," *Microw Opt Technol Lett*. 2018, pp.1–5. https://doi.org/10.1002/mop.31447.
4. Z. Qi, F. Kan, L. Tie-zhu, " Analysis of planar inverted-f antenna using equivalent models," *In IEEE AP-S Int. Symp./USNC/URSI Meeting*, 2005, vol. 3A, pp. 142–145.
5. C. Huynh, W. Stutzman, " Ground plane effects on planar inverted-f antenna (PIFA) performance," *Proc. Inst. Elect. Eng.—Microw., Antennas, Propag.*, 2003, vol. 150, no. 4, pp. 209–213.
6. S. Salama, D. Zyoud, R. Daghlas, A. Abuelhaija, "Design of a Planar Inverted F-Antenna for Medical Implant Communications Services Band," *International Conference on Mathematics, Engineering, Science and Technology 2020, 19-20 SEPT 2020*.
7. S. Salama, D. Zyoud, A. Abuelhaija, "Design of a Dual-Band Planar Inverted F-L Implantable Antenna for Biomedical Applications," *International Conference on Mathematics, Engineering, Science and Technology 2020, 19-20 SEPT 2020*.
8. M. Usluer, B. Cetindere, S. Cumhur Basaran, "Compact implantable antenna design for MICS and ISM band biotelemetry applications," *Microw Opt Technol Lett.*, 2019, pp. 1–7. https://doi.org/10.1002/mop.32185.
9. N. A. Malik, T. Ajmal, P. Sant, and M. Ur-Rehman, "A Compact Size Implantable Antenna for Biomedical Applications," *2020 International Conference on UK-China Emerging Technologies (UCET)*, Glasgow, UK, August 2020.
10. J. Kimi, Y. Rahmat-samii, "Planar Inverted F Antennas on Implantable Medical Devices: Meandered Type Versus Spiral Type," *Microw. Opt. Technol. Letter*, 2006, 48, pp. 567–572.

11. W. Lei, Y. X. Guo, "A Miniaturized Implantable Loop Antenna at MICS and ISM Bands for Biomedical Applications*," 2013 IEEE MTT-S International Microwave Workshop Series on RF and Wireless Technologies for Biomedical and Healthcare Applications (IMWS-BIO)*, Singapore, December 2013.
12. I. A. Shah, M. Zada, and H. Yoo, "Design and Analysis of a Compact-Sized Multiband Spiral-Shaped Implantable Antenna for Scalp Implantable and Leadless Pacemaker Systems," *IEEE Transactions on Antennas and Propagation*, 2019, vol. 67, no. 6, pp. 4230 - 4234.
13. W. C. Liu, F. M. Yeh, and M. Ghavami, "Miniaturized implantable broadband antenna for biotelemetry communication," *MICROWAVE AND OPTICAL TECHNOLOGY LETTERS*, vol. 50, no. 9, September 2008.
14. M. Nachiappan, V. Jeyakumar, T.P. Anand, "Design of compact Implantable Meandered and Sharp Edged Meandered Shaped Antenna for Biomedical Application," *European Journal of Molecular & Clinical Medicine*, vol. 7, no. 11, 2020.
15. R. Alrawashdeh, Y. Huang and P. Cao, "Flexible meandered loop antenna for implants in MedRadio and ISM bands," *ELECTRONICS LETTERS,* vol. 49 no. 24 pp. 1515–1517, November 2013.
16. S. Das, D. Mitra," A Compact Wideband Flexible Implantable Slot Antenna Design with Enhanced Gain," *IEEE Transactions on Antennas and Propagation*, 2018, vol. 66, no. 8, pp. 4309 - 4314.
17. X. Wang, J. Shi, L. Xu, J. Wang, " A Wideband Miniaturized Implantable Antenna for Biomedical Application at HBC Band," *Cross Strait Quad-Regional Radio Science and Wireless Technology Conference (CSQRWC)*, Xuzhou, China, July 2018.
18. strong> R. Pethig, “Dielectric properties of body tissues,” *Clin. Phys. Physiol. Meas.,* 1987, Vol. 8, Suppl. A, 5-12. Printed in Great Britain.
19. strong> A. V. Vorst, A. Rosen, and Y. Kotsuka. RF/Microwave Interaction with Biological Tissues. *A JOHN WILEY & SONS, INC.,* 2006.
20. G. Lovat, P. Burghignoli, F. Capolino, and D. R. Jackson, “Combinations of Low/High Permittivity and/or Permeability Substrates for Highly Directive Planar Metamaterial Antennas,” *IET Microw. Antennas Propag.*, vol. 1, no. 1, pp. 177–183, 2007.
21. S. X. Ta and T. K. Nguyen, “AR Bandwidth and Gain Enhancements of Patch Antenna Using Single Dielectric Superstrate,” *Electronics Letters.*, vol. 53, no. 15, pp. 1015–1017, 2017.
22. S. Das, D. Mitra, B. Mandal and R. Augustine, “Implantable antenna gain enhancement using liquid metal-based reflector,” *Applied Physics A: Materials Science & Processing*, 126(9), 2020. doi:10.1007/s00339-020-03862-2.
23. L. Xu, X. Jin, D. Hua, W. J. Lu, and Z. Duan, “Realization of Circular Polarization and Gain Enhancement for Implantable Antenna,” IEEE Access, vol. 8, 16857–16864. doi:10.1109/ACCESS.2019.2963744.

Figures

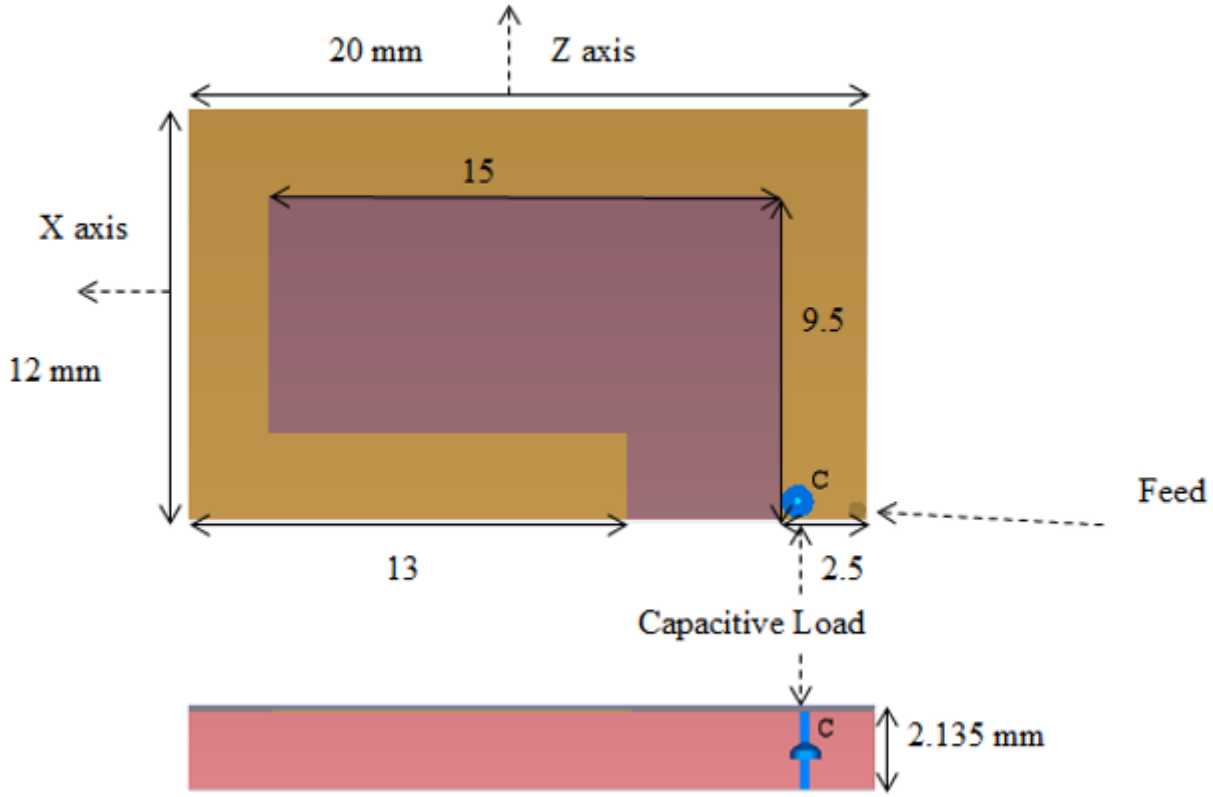

Figure 1

(a) Top view of the capacitive load dual band planar inverted-F implant antenna, and (b) side view of the capacitive load dual band planar inverted-F implant antenna.

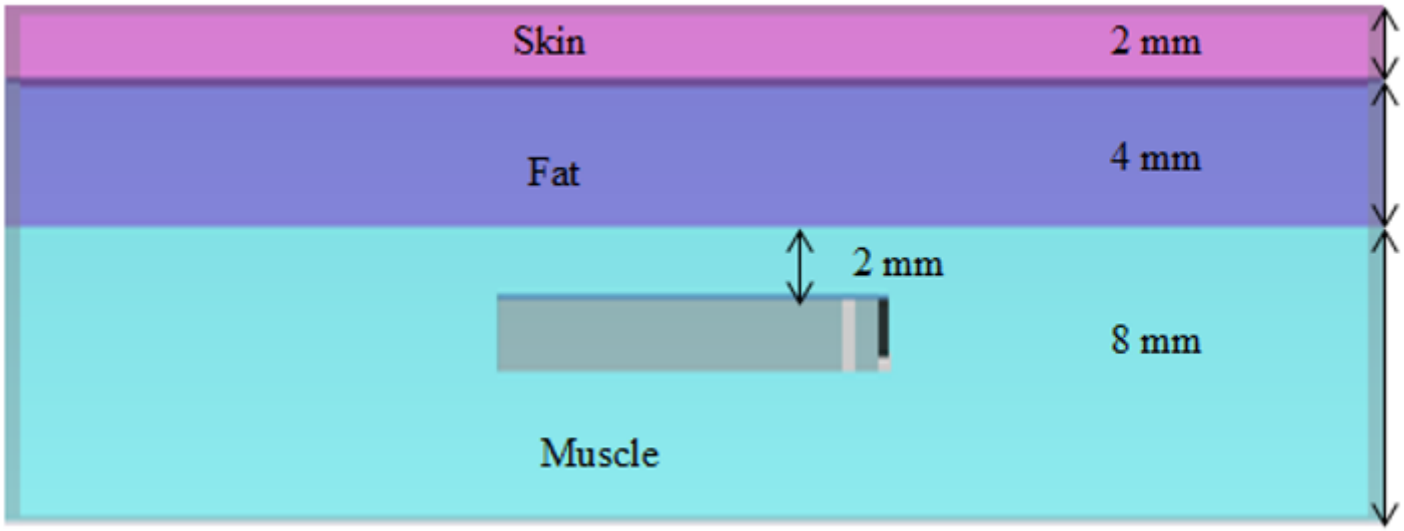

Figure 2

The capacitive load planar inverted-F implant antenna implanted in the muscle layer of a three-layer human tissue model.

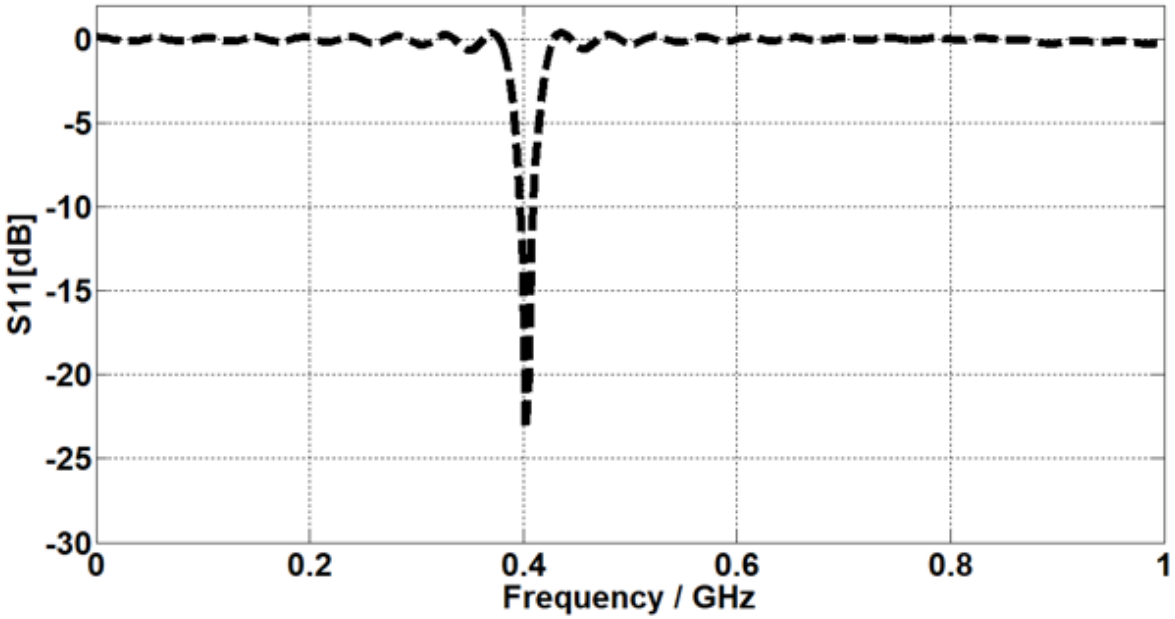

(a)

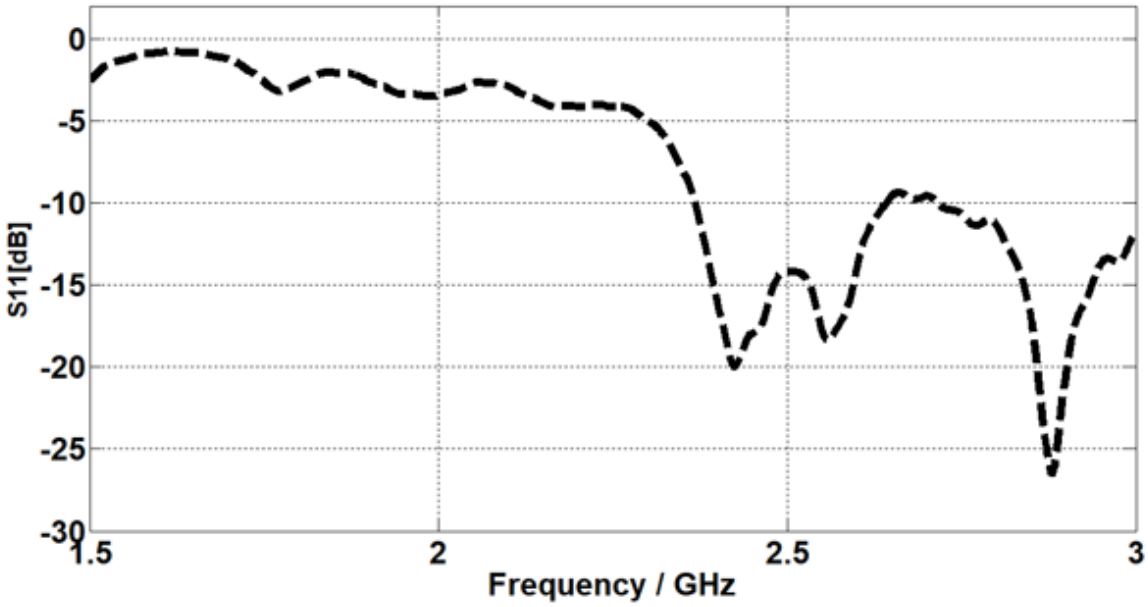

(b)

Figure 3

Simulated return loss of the capacitive load planar inverted-F implant antenna: (a) MICS band, and (b) ISM band.

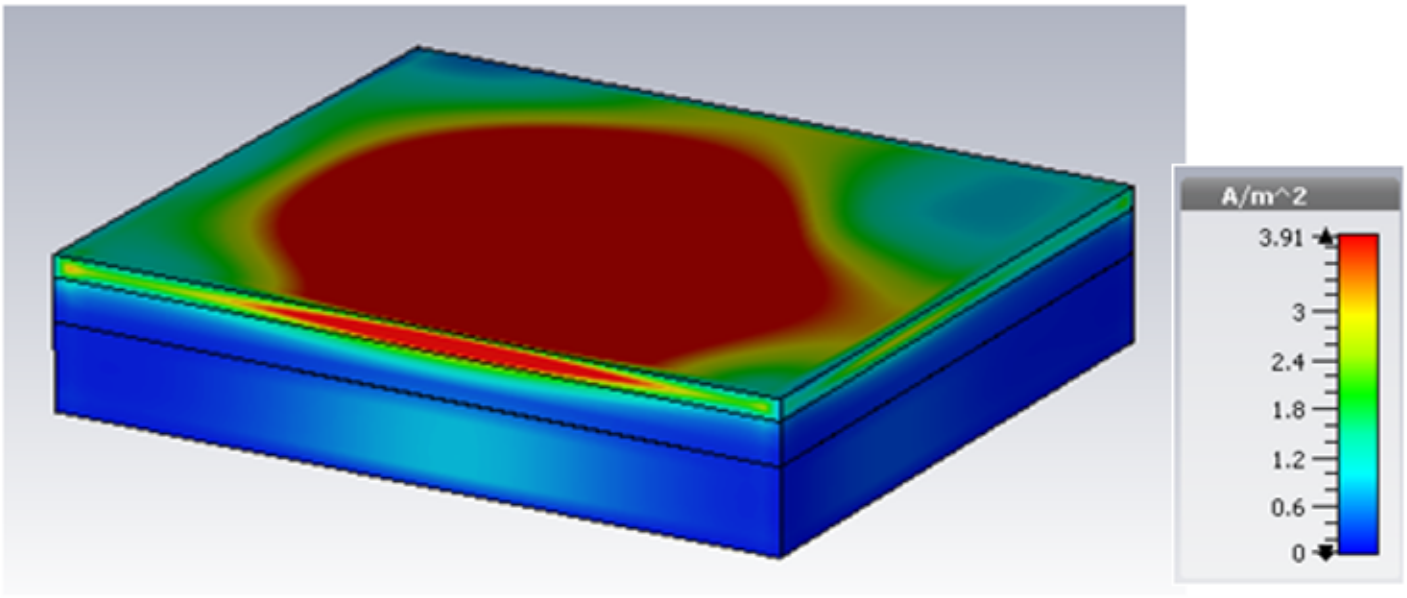

(a)

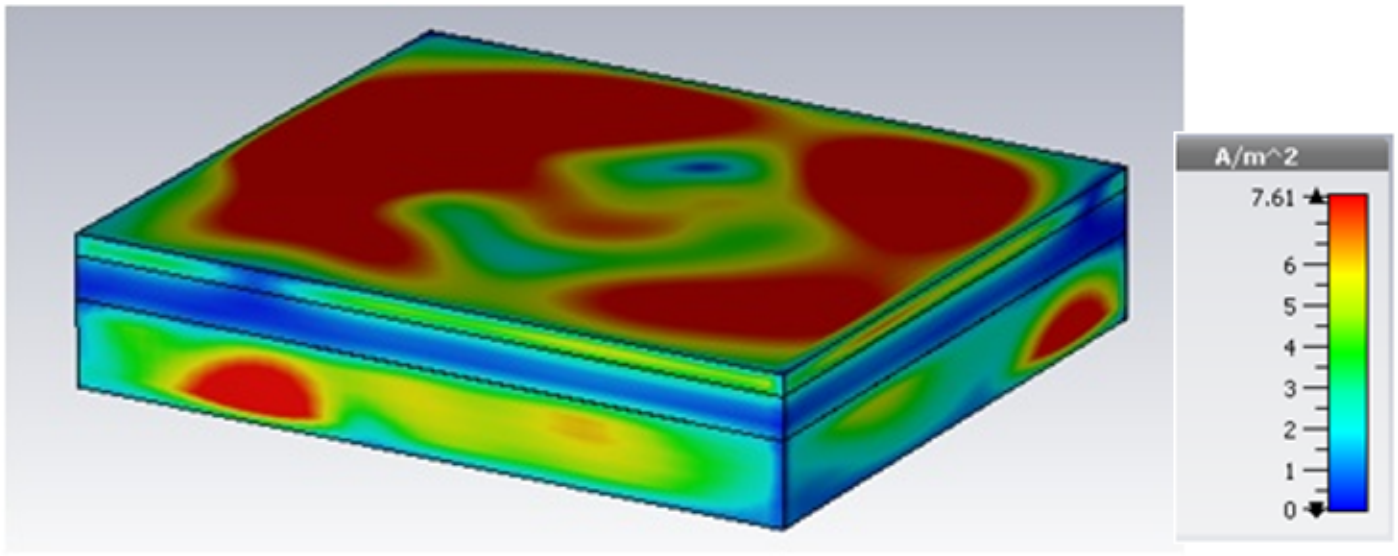

(b)

Figure 4

Simulated current density distribution of the capacitive load planar inverted-F implant antenna at: (a) 402MHz, and (b) 2.42GHz.

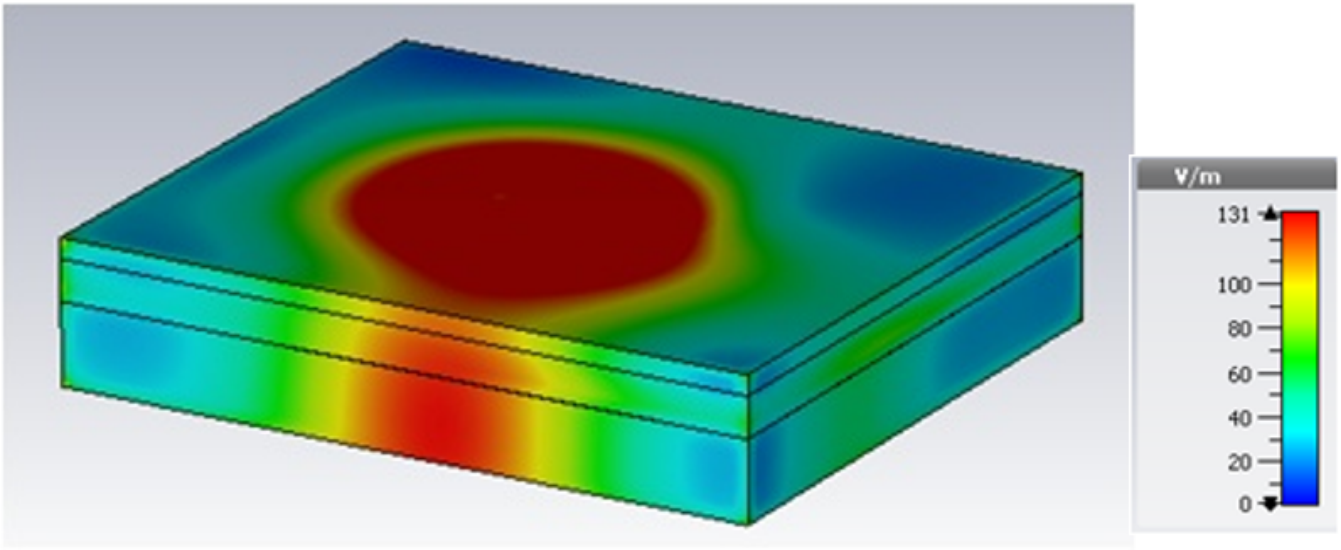

(a)

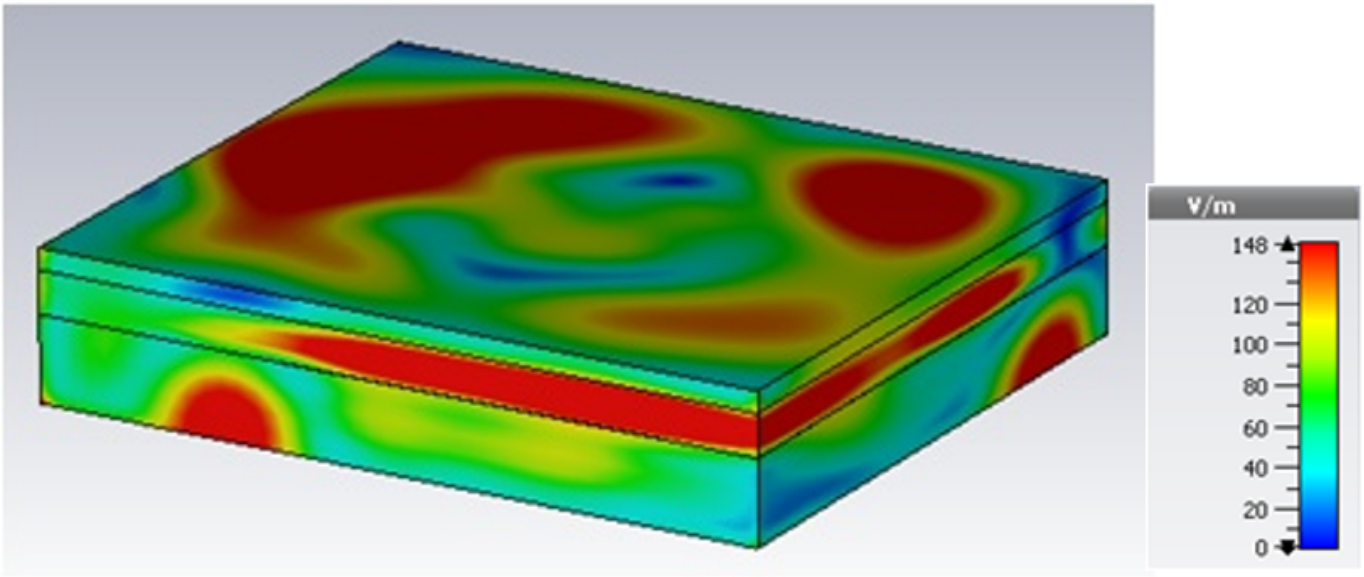

(b)

Figure 5

Simulated electric-field intensity of the capacitive load planar inverted-F implant antenna at: (a) 402MHz, and (b) 2.42GHz.

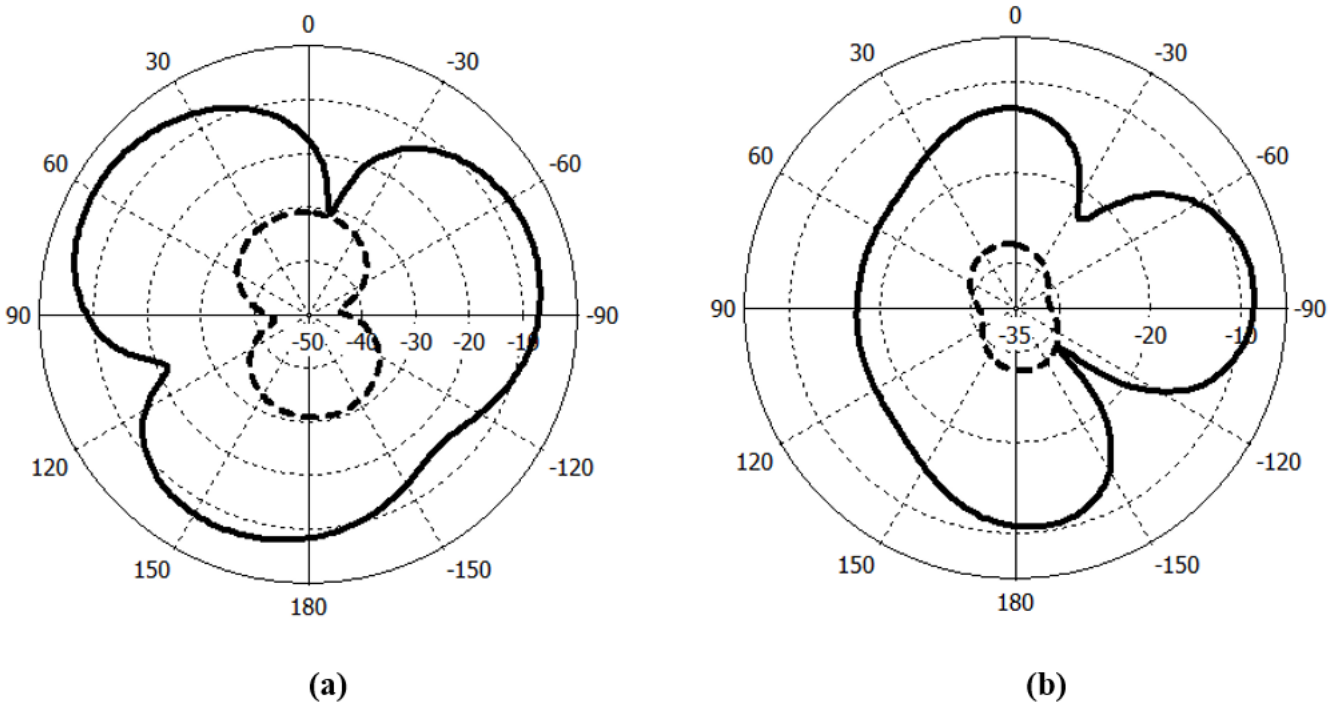

Figure 6

Simulated far-fields of the capacitive load planar inverted-F implant antenna: (a) Azimuth pattern (theta = 90^{o}) at 402 MHz (dash line) and 2.42 GHz (solid line), and (b) Elevation pattern (phi = 0) at 402 MHz (dash line) and 2.42 GHz (solid line).

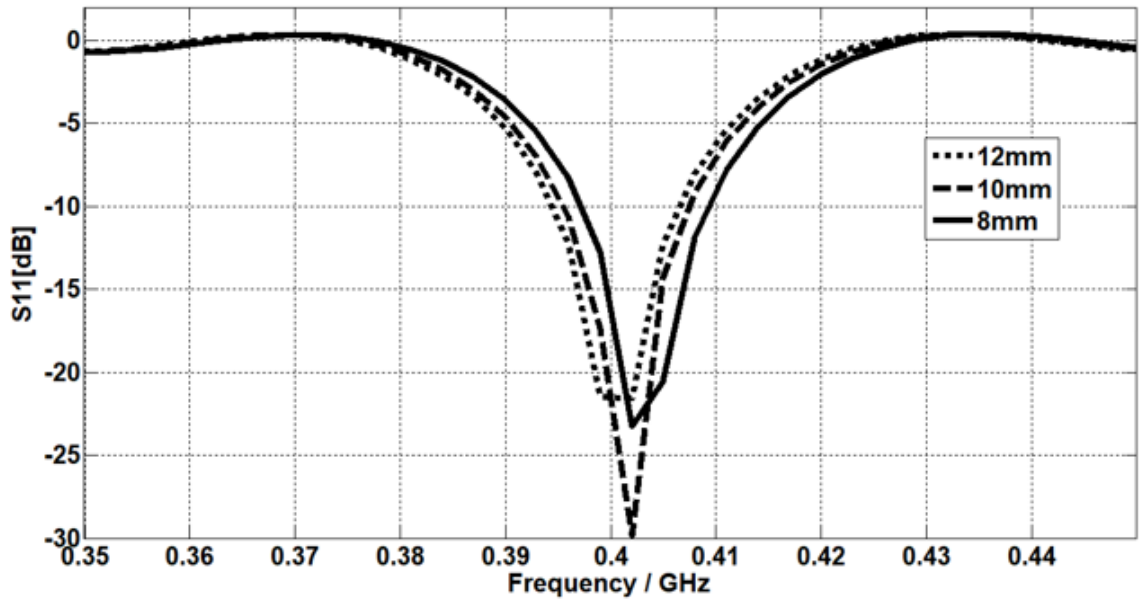

(a)

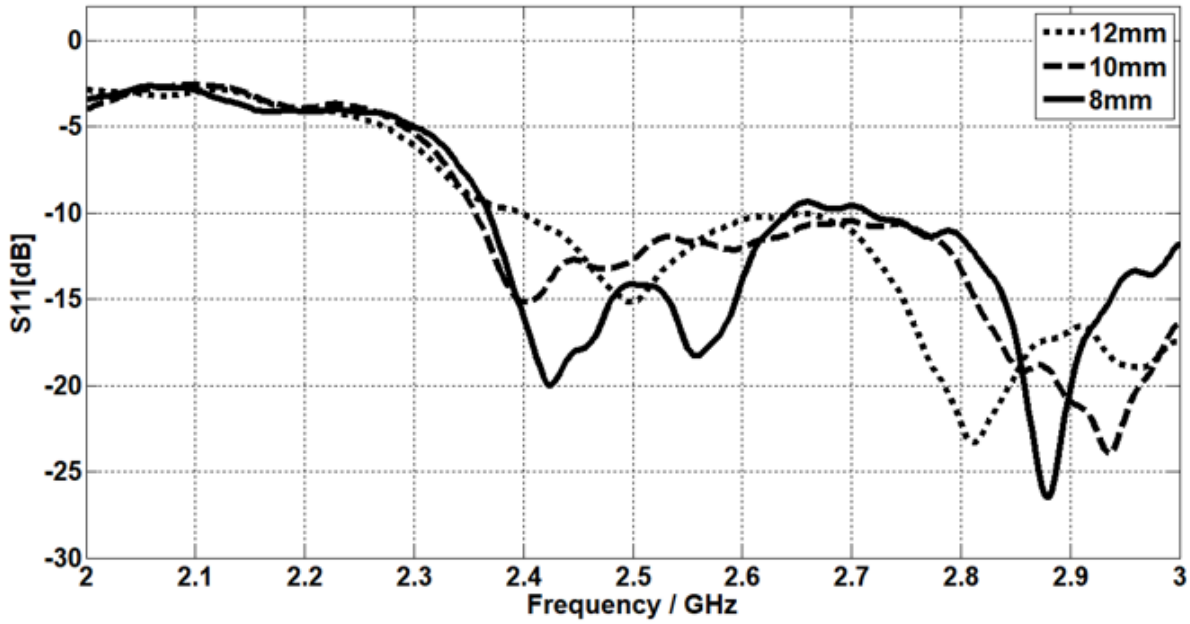

(b)

Figure 7

Simulated return loss at different implantable depths: (a) MICS band, and (b) ISM band.

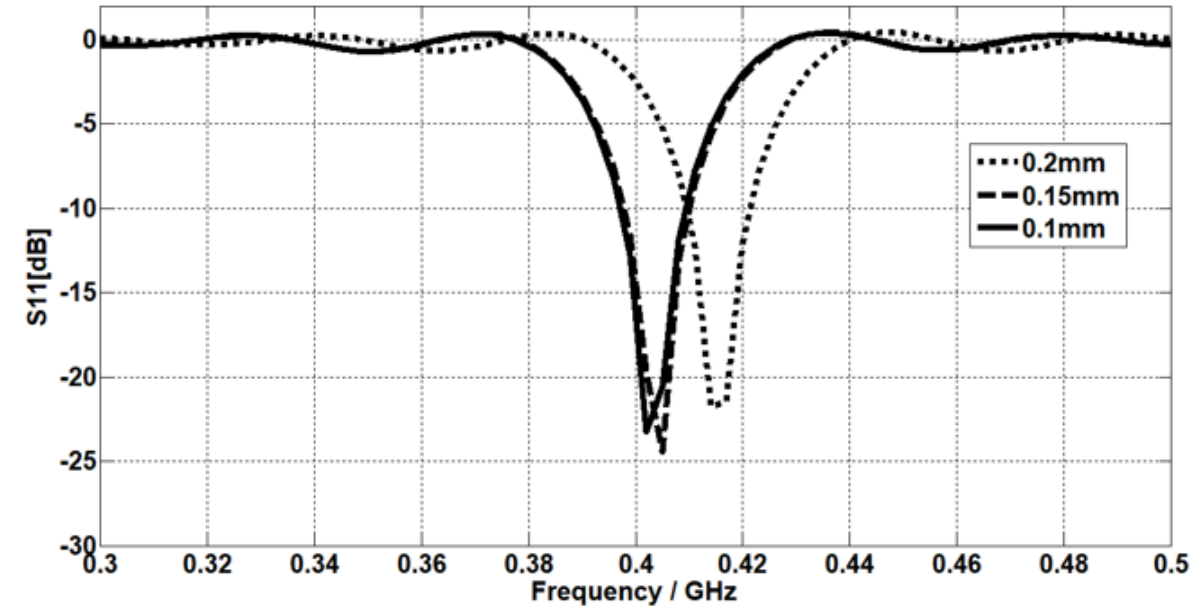

(a)

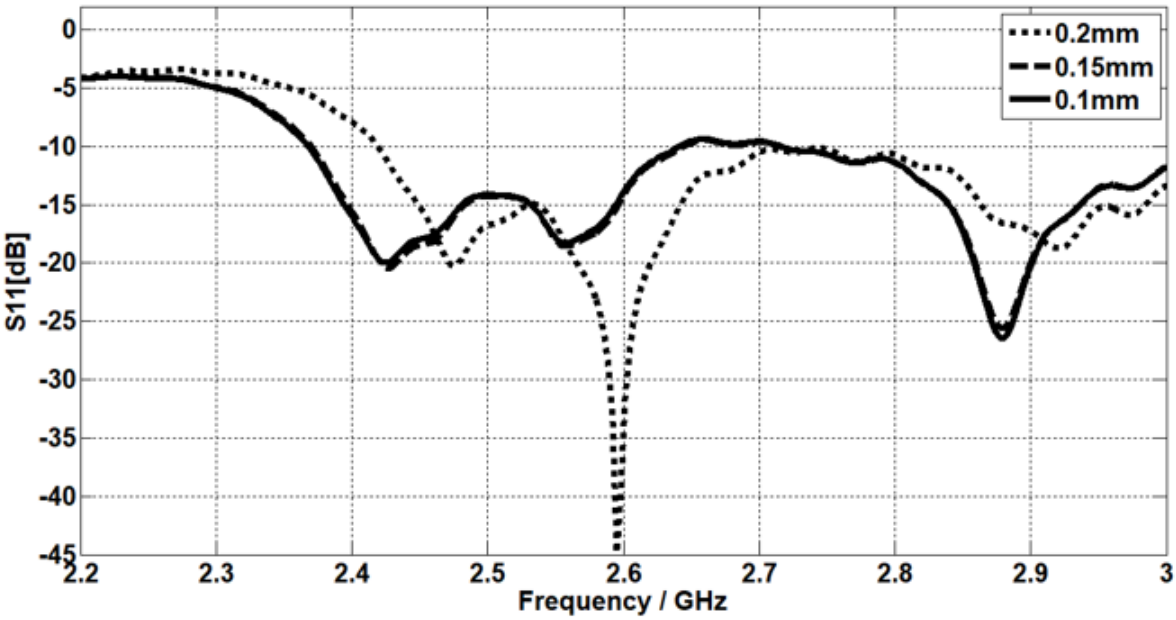

(b)

Figure 8

Simulated return loss at different biocompatible layer thickness: (a) MICS band, and (b) ISM band.